

# Radical Carbon Skeleton Rearrangements: Catalysis by Coenzyme B<sub>12</sub>-Dependent Mutases

Ruma Banerjee\*

Biochemistry Department, University of Nebraska, Lincoln, Nebraska 68588-0664

Received July 30, 2002

## Contents

I. Introduction	2083
II. AdoCbl: A Radical Reservoir	2085
A. Conformation of B <sub>12</sub> in the Active Sites of Carbon Skeleton Isomerases	2085
B. Role of the Histidine Ligand	2086
C. Co–C Force Constant	2087
III. Substrate Radical Generation	2087
A. Kinetic Coupling as a Means of Controlling Reactivity of the Radical Reservoir	2087
B. Quantum Mechanical Tunneling in the Hydrogen-Transfer Steps	2088
C. Detection of Radical Intermediates by EPR Spectroscopy	2088
D. Controlling Radical Trajectories	2089
IV. The Rearrangement Reaction	2090
A. Chemical and Computational Models	2091
B. Comparison of Active Sites of Methylmalonyl-CoA Mutase and Glutamate Mutase	2091
V. Qualitative Free Energy Profiles	2092
VI. Conclusions	2093
VII. Acknowledgment	2093
VIII. References	2093



Ruma Banerjee was born in Calcutta, India, and was raised as an army brat who changed 10 schools before graduating at the age of 15. She received her formal training in botany (B.S. and M.S. from the University of Delhi), biochemistry (Ph.D. from Rensselaer Polytechnic Institute, NY), and biophysics (University of Michigan) before setting out on her own at the University of Nebraska, where she is currently a Willa Cather Professor of Biochemistry and Director of the Redox Biology Center. Her interests range from radical reactions catalyzed by B<sub>12</sub> enzymes to redox regulation and gene–nutrient interactions in controlling homocysteine flux.

tor, described as a “substance of frightening complexity”,<sup>3</sup> has several distinguishing structural attributes. Rings A and D are directly fused in the corrin ring instead of being bridged by a methylene group, and the biosynthetic pathway outfits the cofactor with an

## I. Introduction

The discovery by Barker in 1958 of a biologically active cobalamin, required for the transformation of glutamate to  $\beta$ -methylaspartate, heralded the discovery of a class of radical B<sub>12</sub>-dependent enzymes that catalyze isomerization reactions.<sup>1</sup> The stable cobalt (Co)–carbon bond of 5'-deoxyadenosylcobalamin (AdoCbl) or coenzyme B<sub>12</sub> holds the key to the reactivity of AdoCbl and was revealed by the historical solution of the crystal structure of this cofactor by Hodgkin and co-workers in 1961.<sup>2</sup> AdoCbl is a portly member of the family of tetrapyrrolic-derived macrocycles (Figure 1). The corrin ring of cobalamin is more reduced and hence perhaps more ancient than its structural cousins, chlorin and heme, but it is more oxidized than the nickel-containing corphin ring. This affords the corrin ring some measure of flexibility that may be important in harnessing its reactivity in enzyme-catalyzed reactions. The cofac-

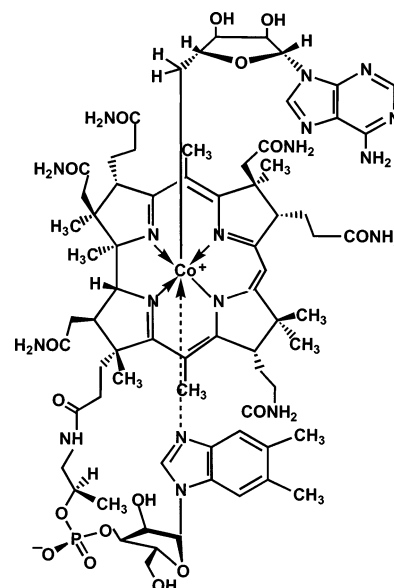
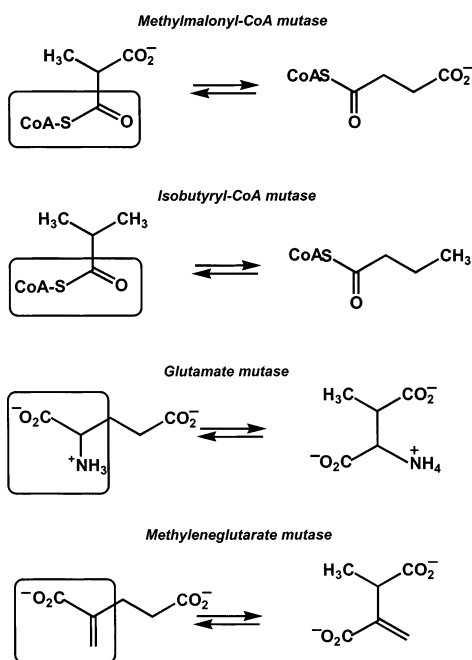


**Figure 1.** Structural formula of AdoCbl.

\* Tel.: (402) 472-2941. Fax: (402) 472-7842. E-mail: rbanerjee1@unl.edu.

### Scheme 1. Reactions Catalyzed by Carbon Skeleton Isomerases



<sup>a</sup> The migrating groups in the forward reactions are boxed.

intramolecular lower axial ligand, dimethylbenzimidazole, which extends from ring D on a side-chain tether. The identity of the base at the terminus of the nucleotide loop varies, and cobalamin refers specifically to a cobamide containing a dimethylbenzimidazole ligand. Other peripheral ornamentations project from the edges of the corrin ring, with acetamide and propionamide side chains crowding the upper and lower faces, respectively. The upper axial ligand is a bulky deoxyadenosyl moiety in AdoCbl and a methyl group in methylcobalamin, the only other biologically active alkylcobalamin.

The reactions catalyzed by AdoCbl-dependent isomerases can be generalized as a 1,2 interchange of a hydrogen atom and a variable group on vicinal carbons. The repertoire of variable groups that are rearranged ranges from heteroatoms (such as  $-\text{OH}$  or  $-\text{NH}_2$ ) to carbon skeleton fragments, and enzymes belonging to the latter subclass are the subject of this review (for other recent reviews, see refs 4–7). There are four AdoCbl-dependent carbon skeleton isomerases known to date: methylmalonyl-CoA mutase, glutamate mutase, methyleneglutarate mutase, and isobutyryl-CoA mutase (Scheme 1). These enzymes play key roles in bacterial fermentation pathways. In contrast to the other three, whose occurrence is restricted to the bacterial kingdom, methylmalonyl-CoA mutase exists in both bacteria and mammals. In the latter, methylmalonyl-CoA mutase serves to funnel catabolites of odd-chain fatty acids and branched-chain amino acids and cholesterol to a useful metabolite, succinyl-CoA. Impairments in this enzyme lead to methylmalonic aciduria, an autosomal recessive disorder associated with aberrations in secondary acid metabolism.<sup>8</sup>

The majority of the bacterial carbon skeleton isomerases are heterodimeric (or higher order oligomers of a heterodimer), and only one of their two

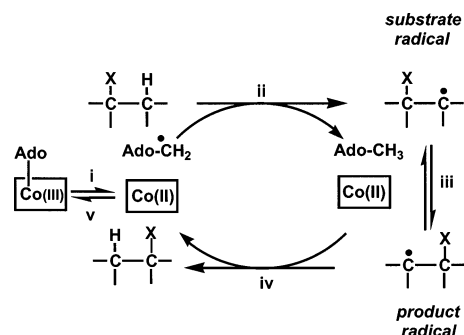


**Figure 2.** Generalized reaction mechanism for AdoCbl-dependent isomerization reactions in which X and H interchange positions via intramolecular and intermolecular pathways, respectively.

subunits binds the cofactor.<sup>9,10</sup> Exceptions are methyleneglutarate mutase<sup>11</sup> and the *Escherichia coli* methylmalonyl-CoA mutase encoded by the *sbm* or “sleeping beauty mutase” gene,<sup>12</sup> which are homodimeric, as is the mammalian methylmalonyl-CoA mutase. The *E. coli* enzyme is normally not expressed due to the absence of a functional promoter, but the recombinant protein has methylmalonyl-CoA mutase activity.<sup>13</sup> This raises the intriguing question as to whether horizontal gene transfer was involved in the exchange of this gene between kingdoms. In this context, it is interesting to note that the megaplasmid, pRmeSU47b, from *Sinorhizobium meliloti* encodes an apparently homodimeric methylmalonyl-CoA mutase.<sup>14</sup>

In three of the four carbon skeleton isomerases, the migrating group involves an  $\text{sp}^2$ -hybridized carbon. In contrast, glutamate mutase catalyzes the migration of an  $\text{sp}^3$ -hybridized glycol moiety (Scheme 1). These chemically challenging transformations are realized by deployment of radical chemistry, which explains their dependence on AdoCbl, a cofactor which functions as a reversible radical repository. A minimal catalytic scheme is presented in Figure 2, in which homolytic cleavage of the Co–carbon bond initiates the radical roulette by generating a metal-centered cob(II)alamin radical and a carbon-centered deoxyadenosyl radical (dAdo•) (step i). The deoxyadenosyl radical, a high-energy intermediate that has so far evaded detection, generates a substrate-centered radical by abstraction of a hydrogen atom (step ii). Evidence for the intermolecular transfer of the migrating hydrogen atom from substrate to cofactor was first provided by tritium labeling studies in the AdoCbl-dependent enzyme, diol dehydratase.<sup>15</sup> In contrast, the variable carbon skeleton moiety undergoes an intramolecular migration and yields a product radical (step iii). Reabstraction of a hydrogen atom from deoxyadenosine (step iv), followed by recombination of the cofactor radicals (step v), cob(II)alamin and dAdo•, complete passage through a single catalytic turnover.

Despite the absence of overall sequence homology between methylmalonyl-CoA mutase and glutamate mutase, the two enzymes exhibit a striking resemblance to each other at a three-dimensional level (Figure 3). Methylmalonyl-CoA mutase from *Propionibacterium shermanii* is an  $\alpha\beta$  heterodimer in which the  $\alpha$  subunit houses the cobalamin-binding

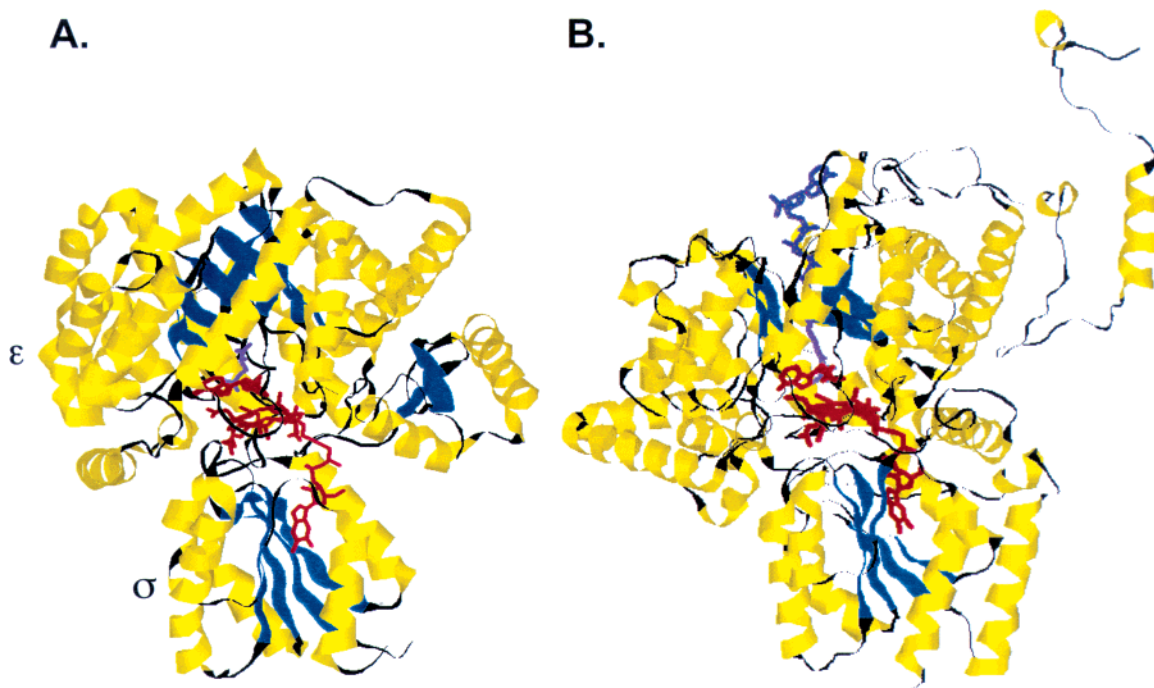


**Figure 3.** Comparison of the overall architectures of glutamate mutase and methylmalonyl-CoA mutase. (A) In glutamate mutase, a heterodimeric unit ( $\epsilon$  and  $\sigma$  subunits) of a heterotetrameric ( $\epsilon_2\sigma_2$ ) structure is shown containing bound AdoCbl (in red) and glutamate (in purple). The figure was generated from the PDB file 1I9C. (B) Only the  $\alpha$  subunit of the  $\alpha\beta$  heterodimer is shown with bound AdoCbl (in red) and the substrate, methylmalonyl-CoA (in purple), piercing through the TIM barrel. The figure was generated from the PDB file 4REQ.

domain and the active site. This subunit alone is structurally analogous to one  $\sigma/\epsilon$  unit in the heterotetrameric  $\sigma_2/\epsilon_2$  glutamate mutase (Figure 3A). The  $\alpha/\beta$  B<sub>12</sub>-binding domain ( $\sigma$  subunit in glutamate mutase and residues  $\alpha 597$ – $\alpha 728$  in methylmalonyl-CoA mutase) has a Rossmann-like fold.<sup>16,17</sup> The substrate-binding domain is packed on the upper face of cobalamin and is an  $(\alpha/\beta)_8$  or TIM barrel domain in both enzymes. In methylmalonyl-CoA mutase, the substrate enters the active site by piercing through the TIM barrel, in a fashion that is apparently unique (Figure 3B).<sup>16</sup> This is accompanied by a substantial conformational change as the barrel snaps in around the CoA tail of the substrate, effectively sealing off the active site from the exterior.<sup>18,19</sup> The impact of this motion is evident on an active-site residue, Y89, which is perched above the adenine ring in the absence of substrate but moves in toward the corrin ring in the presence of substrate, and it may play a key role in facilitating the homolysis and/or kinetic coupling step(s).<sup>18</sup>

## II. AdoCbl: A Radical Reservoir

The Co–carbon bond is a water-stable organometallic bond, which can be formulated as a carbanion coordinated to a trivalent cobalt. The role of the cofactor as a reversible free radical reservoir hinges on the relative weakness of its Co–carbon bond, and the bond dissociation energy (BDE), estimated to be  $\sim 30$  kcal mol<sup>-1</sup> for “base-on”<sup>20</sup> AdoCbl,<sup>21</sup> is significantly lower than for most covalent bonds in organic molecules. Dissociation of the lower axial base, dimethylbenzimidazole, by protonation ( $pK_a = 3.7^{22}$ ) results in the “base-off” conformation and alleviation of trans effects with a corresponding increase in the

Co–carbon BDE to 34.5 kcal mol<sup>-1</sup>.<sup>23</sup> In solution, the rate constant for homolysis of the Co–carbon bond is estimated to be  $\sim 3.8 \times 10^{-9}$  s<sup>-1</sup> at 37 °C, corresponding to a half-life of 5.8 years. In contrast, the rate constants for the carbon skeleton isomerases are in the range of  $\sim 10$ – $100$  s<sup>-1</sup>,<sup>10,24</sup> corresponding to half-lives of a few milliseconds and translating minimally to a  $10^{12 \pm 2}$ -fold rate acceleration in the enzyme-catalyzed homolytic cleavage reaction. Elucidation of the catalytic tactics employed to effect this hefty unimolecular rate acceleration has spurred debate and fueled a significant body of model studies.

## A. Conformation of B<sub>12</sub> in the Active Sites of Carbon Skeleton Isomerases

The steric and electronic contributions of the lower axial ligand, dimethylbenzimidazole, in modulating the strength and therefore the reactivity of the trans Co–carbon bond, and the role of the puckered corrin ring in transmitting these effects, have been the focus of many model studies.<sup>25–30</sup> However, in methylmalonyl-CoA mutase<sup>16,31</sup> and in glutamate mutase,<sup>17,32</sup> spectroscopic and/or structural studies have revealed that a significant conformational change accompanies docking of the cofactor in the respective active sites. Thus, AdoCbl is lodged in a “base-off” form in which the endogenous base, dimethylbenzimidazole, is buried in a relatively hydrophobic cavity and separated by  $> 10$  Å from the cobalt (Figure 4). An active-site histidine residue replaces the intramolecular base as the lower axial ligand, resulting in retention of the six-coordinate state. The ligating histidine resides in a conserved motif, DXHXXC<sup>33</sup> (Figure 4A), a sequence that is also present in methyleneglutarate mutase and in isobutyryl-CoA

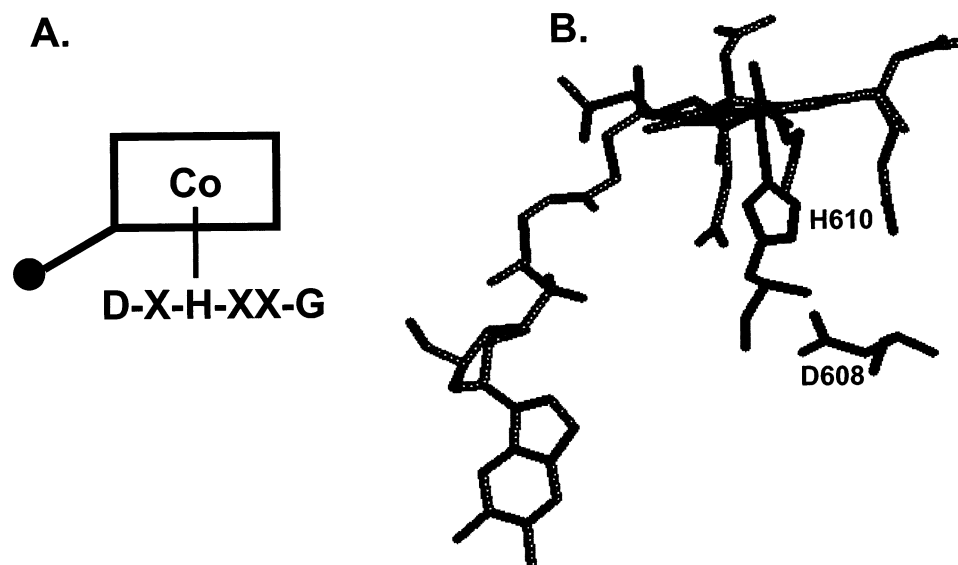


**Figure 4.** “His-on” conformation of cobalamin in the Class I family of AdoCbl-dependent enzymes. (A) Schematic depiction of the ligand replacement that accompanies  $B_{12}$  binding in this class of enzymes. A histidine residue in the conserved DXHXXG motif replaces the endogenous dimethylbenzimidazole ligand. (B) Conformation of cobalamin bound to the active site of the *P. shermanii* methylmalonyl-CoA mutase along with the other triad residues, H610 and D608.

mutase, leading to the prediction that these too belong to the “his-on” or Class I subfamily of AdoCbl-dependent enzymes. In contrast, in the “dimethylbenzimidazole-on” or Class II subfamily, the bound cofactor retains its intramolecular base as the lower axial ligand. Members of this latter subfamily include diol dehydratase,<sup>34</sup> ethanolamine ammonia lyase,<sup>35</sup> and ribonucleotide reductase.<sup>36</sup>

The active sites of glutamate mutase and methylmalonyl-CoA mutase extend their grasps over AdoCbl via numerous electrostatic interactions.<sup>16,17</sup> The peripheral propionamide and acetamide functionalities on the corrin ring are the foci of multiple interactions (either directly or via water bridges) with backbone amides and amino acid side chains in the active site. In contrast, the dimethylbenzimidazole loop is lodged in a hydrophobic cavity without any direct hydrogen bonds with the protein in glutamate mutase and in methylmalonyl-CoA mutase and with only a few ionic interactions between the nucleotide and the respective proteins.<sup>16,17</sup> The deoxyadenosyl moiety of AdoCbl is parked over pyrrole ring B in methylmalonyl-CoA mutase<sup>18</sup> and in glutamate mutase<sup>37</sup> rather than ring C, as in the free cofactor.

## B. Role of the Histidine Ligand

The effects of histidine versus dimethylbenzimidazole ligation to cobalt have been explored in model studies using the cofactor analogue, AdoCbi,<sup>20</sup> in which the nucleotide loop is truncated, leading perforce to a “base-off” conformation. AdoCbi in the presence of *N*-methylimidazole (N-MeIm) was used to mimic the “his-on” class of isomerases.<sup>38</sup> These studies revealed that N-MeIm significantly reduces the proportion of Co–carbon bond homolysis from  $\geq 98\%$  in AdoCbl to  $\sim 50\%$  in the AdoCbi:N-MeIm complex, with the remainder occurring via the heterolytic route. In addition, N-MeIm accelerated Co–carbon bond homolysis in AdoCbi by a factor of 8 relative to AdoCbl, but heterolysis was enhanced by

a factor of 350! These model studies suggest that suppression of the nonbiological heterolytic pathway in the “his-on” class may be an important issue for the enzymes.

The role of imidazole ligation has been addressed in a physiological context in several of the carbon skeleton isomerases. The cobalt–histidine interaction is a component of an electrostatic triad, which includes the aspartate in the DXHXXG motif (Figure 4). In glutamate mutase, mutation of the coordinating histidine, H15, to glycine or glutamine raises the apparent  $K_d$  for AdoCbl by  $>50$ -fold and diminishes  $k_{cat}$   $\sim 10^3$ -fold.<sup>39</sup> In methyleneglutarate mutase, mutation of the histidine ligand, H485, to glutamine results in a 4000-fold decrease in  $k_{cat}$ ; however, the effect on cofactor binding has not been reported.<sup>40</sup> In methylmalonyl-CoA mutase, mutation of H610 to alanine and asparagine results in a 5000- and 40000-fold diminution in  $k_{cat}$ , respectively, and a profoundly weakened affinity for the cofactor, AdoCbl.<sup>41</sup> However, binding of the truncated cofactor missing the nucleotide tail, AdoCbi, is significantly less affected.

On the surface, these results suggest an important role for the histidine residue in weakening the Co–carbon bond. However, catalytic turnover of wild-type methylmalonyl-CoA mutase reconstituted with the cofactor analogue, AdoCbi-GDP,<sup>20</sup> is only mildly affected, despite the cofactor adopting a “his-off” conformation in the active site.<sup>42</sup> Thus,  $k_{cat}$  for the enzyme is reduced by a factor of 4 compared to that for the native cofactor, AdoCbl. The overall deuterium isotope effect in the presence of AdoCbi-GDP ( $PV = 7.2 \pm 0.8$ ) is comparable to that observed in the presence of AdoCbl ( $5.0 \pm 0.6$ ), which indicates that the hydrogen-transfer steps in this reaction are not significantly affected by the absence of histidine ligation.

These results suggest that the cofactor tail may be important in organizing a high-affinity cofactor-binding site, possibly by correctly orienting the triad

residues to permit electrostatic interactions, and that the primary role of the histidine is in cofactor binding rather than in catalysis.<sup>42,43</sup> This model is supported by structural comparisons of the B<sub>12</sub>-binding domain of glutamate mutase in the presence and in the absence of B<sub>12</sub>.<sup>17,44</sup> This domain is largely preorganized, with the exception of a stretch of sequence that adopts an  $\alpha$  helix in the presence of B<sub>12</sub> and is disordered in its absence. This helix enjoys a critical location leading directly from the loop on which the triad residues, histidine and aspartate, reside.

### C. Co–C Force Constant

While the relative weakness of the Co–carbon bond with a BDE of 30 kcal mol<sup>-1</sup><sup>21</sup> is key to the utility of AdoCbl as a reversible radical reservoir, it also holds perils for enzymes that utilize this cofactor. Significant ground-state destabilization of the bond in the holoenzyme, i.e., in the absence of substrate, would risk dissipation of the radicals in inadvertent side reactions leading to enzyme inactivation. On the other hand, the enzymes must orchestrate a very significant 17 kcal mol<sup>-1</sup> or so destabilization of the Co–carbon bond, corresponding to the estimated trillion-fold rate acceleration which is observed during catalysis. This leads to the question of how the dormant radical reservoir of the bound cofactor is controlled to initiate radical reactions during turnover. While model studies have illuminated the potential for a mechanochemical trigger mechanism, whereby an upward flexing of the corrin ring would lead to steric crowding, thereby weakening the organometallic bond,<sup>27,30,45–47</sup> experimental evidence for ground-state destabilization in these enzymes has been lacking. Resonance Raman studies have been useful in probing the relative force constants of the Co–carbon bond in free and enzyme-bound AdoCbl in methylmalonyl-CoA mutase.<sup>48–51</sup> Isotope editing permitted identification of  $\nu(\text{Co–C})$  at 424 cm<sup>-1</sup> in free versus 420 cm<sup>-1</sup> in mutase-bound AdoCbl.<sup>49</sup> The minor frequency downshift observed for the bound versus the free cofactor translates to an estimated  $\sim 0.5$  kcal mol<sup>-1</sup> weakening of the Co–carbon bond in the methylmalonyl-CoA mutase active site, consistent with the notion that the labilization occurs largely upon binding of substrate. Resonance Raman spectra for AdoCbl bound to glutamate mutase have been reported recently, although the  $\nu(\text{Co–C})$  of the free and bound cofactor were assumed based on the values reported for methylmalonyl-CoA mutase and not assigned independently.<sup>52</sup> However, the spectra of free and glutamate mutase-bound AdoCbl were similar in this region, consistent with the absence of detectable weakening of the Co–carbon bond in the ground state.

In addition to the Co–carbon bond stretching vibration, three other resonance Raman bands arising from the Co-bound adenosine, including the Co–C–C angle bend, a 5'-C-coupled ribose deformation, and a hindered rotation of the adenosine about the Co–carbon bond, could be detected via isotope editing in methylmalonyl-CoA mutase.<sup>48</sup> Slow substrates or inhibitors on one hand and product on the other were used to mimic the substrate- and product-bound

states, respectively, of the enzyme and found to affect the resonance Raman enhancement pattern differentially. These changes are indicative of Co-Ado tilting to a small extent in the resting enzyme and to a larger extent in the substrate-bound state and suggest that this steric change is a contributor to the activation of the Co–carbon bond.<sup>48</sup>

## III. Substrate Radical Generation

### A. Kinetic Coupling as a Means of Controlling Reactivity of the Radical Reservoir

Although significant ground-state destabilization of the Co–carbon bond in the bound cofactor is not supported experimentally, cleavage of this bond in the absence of substrate is indicated by stereochemical scrambling of deuterium at the C5' position of AdoCbl in methylmalonyl-CoA mutase.<sup>53</sup> However, the homolysis product, cob(II)alamin, is not detected by either UV–visible or EPR spectroscopy in the absence of substrate, indicating that the homolysis equilibrium greatly favors geminate recombination. Insights into how the equilibrium is tipped in favor of forward propagation of the organic radical during catalysis have emerged from measurements of the isotope effect on the homolysis reaction under pre-steady-state conditions. In both methylmalonyl-CoA mutase<sup>24</sup> and glutamate mutase,<sup>54</sup> deuterium labeling of substrates results in deceleration of the Co–carbon bond cleavage rate by  $>20$ -fold. This unusual sensitivity of the cofactor chemistry to isotopic substitution in the substrate has been interpreted as evidence for kinetic coupling of the homolysis and substrate radical generation steps in which the unfavorable equilibrium for homolysis is shifted to the right by coupling to the favorable equilibrium governing substrate radical generation (Figure 5).<sup>24</sup>

In methylmalonyl-CoA mutase, both the 5'-deoxyadenosyl radical and the methylmalonyl-CoA radical are primary in nature; however, the methylmalonyl-CoA radical is beta to a carboxylate (Scheme 3). A recent QM/MM study modeling the initial steps of

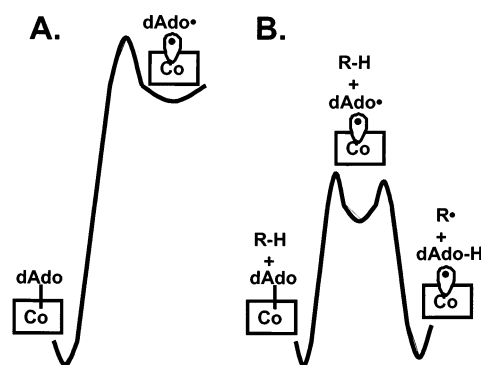
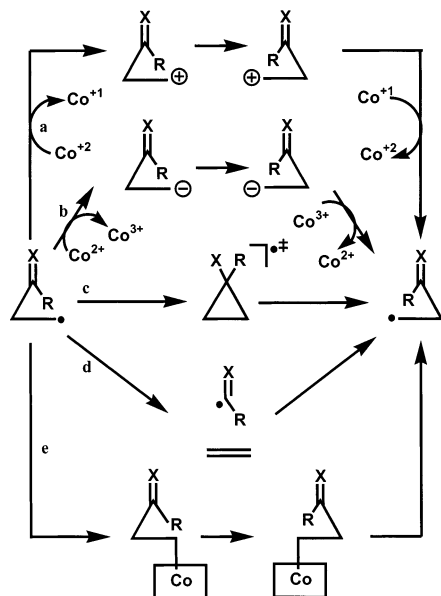


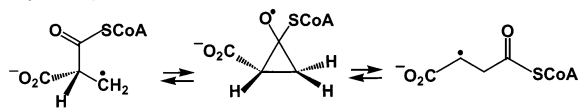
**Figure 5.** Comparison of the qualitative free energy profiles of the uncatalyzed and methylmalonyl-CoA mutase-catalyzed Co–carbon homolysis steps. (A) Thermolysis of free AdoCbl is characterized by a large enthalpic barrier and an unfavorable equilibrium. (B) The enzyme-catalyzed step is characterized by a significantly lower activation barrier ( $\Delta\Delta G^\ddagger = 13$  kcal mol<sup>-1</sup> at 37 °C) and a more favorable equilibrium brought about by kinetic coupling of the homolysis and substrate hydrogen atom abstraction steps.

### Scheme 2. Alternative Pathways for Rearrangement of an $sp^2$ -Hybridized Carbon

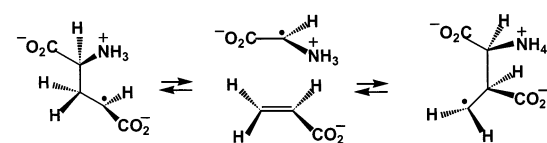


### Scheme 3. Plausible Rearrangement Pathways for Methylmalonyl-CoA Mutase and Glutamate Mutase

#### Methylmalonyl-CoA mutase



#### Glutamate mutase



the methylmalonyl-CoA mutase-catalyzed reaction predicts that formation of the substrate radical from the deoxyadenosyl radical is exothermic and that deprotonation of the carboxylic acid stabilizes the substrate radical by  $\sim 2.5$  kcal mol $^{-1}$ .<sup>55</sup> The guanidino group of R207 makes a two-pronged hydrogen-bonding contact with the substrate carboxylate in methylmalonyl-CoA mutase (Figure 6A,C) and is likely to play a role in modulating the relative stabilities of the substrate and product radicals that are beta and alpha to the carboxylate, respectively.

In glutamate mutase, the substrate glutamyl radical is secondary and alpha to the carboxylate, whereas the product methylaspartyl radical is primary and beta to the carboxylate (Scheme 3). The substrate is laced in by an intricate network of hydrogen bonds, including interactions with three arginine residues<sup>17</sup> that may be similarly important in affecting the stabilities of the radical intermediates (Figure 6). The calculated C–H BDE in models of 5'-deoxyadenosine is  $\sim 100$  kcal mol $^{-1}$ , and those for glutamate and methylaspartate are 92 and  $\sim 100$  kcal mol $^{-1}$ , respectively.<sup>56</sup> Thus, hydrogen atom abstractions in the forward (from glutamate) and reverse (from methylaspartate) directions are predicted to be exothermic ( $\sim 8$  kcal mol $^{-1}$ ) and thermoneutral, respectively.

Co–carbon bond homolysis is rapid and not rate limiting in either methylmalonyl-CoA mutase<sup>24</sup> or

glutamate mutase.<sup>54</sup> The thermodynamic parameters governing the enzyme-catalyzed homolysis reaction have been reported only for methylmalonyl-CoA mutase among the carbon skeleton isomerases.<sup>57</sup> The enzyme-catalyzed homolysis reaction is characterized by the following parameters:  $\Delta H^\ddagger = 18.8 \pm 0.8$  kcal mol $^{-1}$ ,  $\Delta S^\ddagger = 18.2 \pm 0.8$  cal mol $^{-1}$  K $^{-1}$ , and  $\Delta G^\ddagger = 13.1 \pm 0.6$  kcal mol $^{-1}$  at 37 °C. In contrast, the thermolysis reaction in solution is characterized by the following parameters:  $\Delta H^\ddagger = 34.5 \pm 0.8$  kcal mol $^{-1}$ ,  $\Delta S^\ddagger = 14 \pm 1$  cal mol $^{-1}$  K $^{-1}$ , and  $\Delta G^\ddagger = 30.2$  kcal mol $^{-1}$  at 37 °C.<sup>21</sup> Therefore, the enzymatic enhancement of the homolysis reaction is achieved by a sizable lowering of the activation barrier of 17.1 kcal mol $^{-1}$  (Figure 5).

### B. Quantum Mechanical Tunneling in the Hydrogen-Transfer Steps

While the isotopic sensitivity of the homolytic cleavage reaction is explained by kinetic coupling, the magnitude of the isotopic discrimination is not. Minimally, the reaction involves two hydrogen-transfer steps as a hydrogen atom migrates from the substrate to deoxyadenosine before being returned to product. The overall kinetic isotope effects on these reactions, where measured, are normal and lie within the range predicted for semiclassical behavior.<sup>58–61</sup> In contrast, aberrantly large isotope effects are associated with the coupled homolysis/substrate radical generation steps in methylmalonyl-CoA mutase<sup>24</sup> and glutamate mutase,<sup>54</sup> suggestive of nuclear tunneling. An Arrhenius analysis of the temperature dependence of the isotope effect has been reported for methylmalonyl-CoA mutase.<sup>62</sup> The difference in activation energies for C–H versus C–D and the isotope effect on the Arrhenius preexponentials exhibit large deviations from those predicted for a semiclassical, over-the-barrier transfer pathway and provide strong evidence for quantum mechanical tunneling.

A theoretical evaluation of the kinetic isotope effect on the first hydrogen-atom-transfer step catalyzed by methylmalonyl-CoA mutase has been reported using multidimensional tunneling correction at the zero curvature level.<sup>55</sup> The computed values are in close agreement with the experimental ones and suggest that the recombination step proceeds with an activation energy close to zero.

### C. Detection of Radical Intermediates by EPR Spectroscopy

A mechanistic feature common to the reactions catalyzed by AdoCbl-dependent isomerases is the intermediacy of radical pair species in which the partner radicals are organic and metallic, respectively (Figure 2). This mechanistic tenet is supported by visualization of radical species by EPR spectroscopy. In glutamate mutase, methyleneglutarate mutase, and methylmalonyl-CoA mutase, novel axial EPR spectra are observed when the enzyme is trapped under steady-state turnover conditions.<sup>9,63–66</sup> In methylmalonyl-CoA mutase, addition of substrate leads to the appearance of a spin-coupled EPR

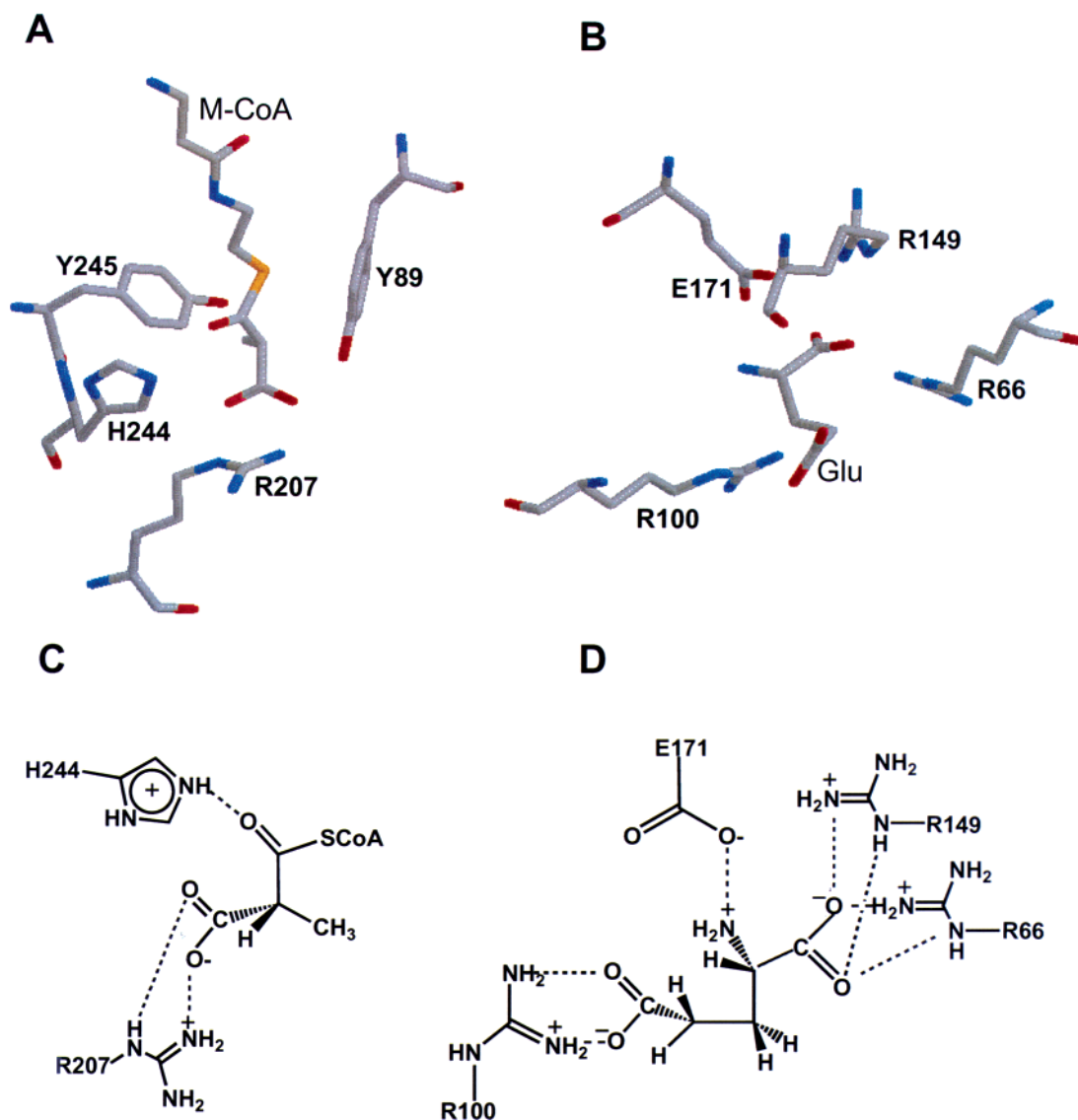


**Figure 6.** Active site residues in methylmalonyl-CoA mutase and glutamate mutase. (A) A portion of the substrate, methylmalonyl-CoA, is shown nestled by polar active-site residues, Y89, R207, H244, and Y245. (B) The active site of glutamate mutase with residues R66, R100, R149, and E171 surrounding glutamate are shown. The electrostatic interactions between the substrate and active-site residues shown in A and B are depicted schematically in C and D.

spectrum (Figure 7).<sup>63,64,67</sup> A power saturation analysis of the EPR spectrum reveals complexity and the presence of two signals, a slow-relaxing species A and a fast-relaxing species B, with effective  $g'$  values of 2.11 and 2.14, respectively, each with a cobalt hyperfine splitting value of 50 G.<sup>64</sup> The spectra could be reasonably well simulated using parameters for cob(II)alamin interacting via electron–electron exchange and dipolar couplings with a carbon-centered radical species.<sup>68</sup> Similar but not identical spectra are observed in the presence of substrate analogues and inhibitors.<sup>69</sup>

Addition of substrate to glutamate mutase leads to the development of an EPR signal that is similar to the one first reported for methylmalonyl-CoA mutase,<sup>63</sup> with a  $g'$  value of 2.1 and a cobalt hyperfine splitting value of 55 G.<sup>9</sup> Selective isotope labeling of glutamate and simulations of the resulting spectra provided strong evidence for the predominance of the 4-glutamyl radical separated from the cobalt radical by a distance of  $6.6 \pm 0.9$  Å.<sup>65</sup> This distance can be

accommodated within the active site in the crystal structure of glutamate mutase.<sup>17</sup>

#### D. Controlling Radical Trajectories

Controlled propagation of the organic radical from the deoxyadenosyl moiety to the substrate and back demands exquisite conformational control so that side reactions are averted. From the EPR studies described above, it can be inferred that the distance between the initially formed radical pair, dAdo<sup>•</sup> and cob(II)alamin, widens in the subsequent substrate–cob(II)alamin radical pair. This leads to the question of how the radicals are shielded from the danger of side reactions as they traverse these distances in active sites lined with polar residues. Structural studies on glutamate mutase have provided fascinating glimpses into the solution adopted by that enzyme,<sup>37</sup> which may well be a general mechanism for the carbon skeleton isomerases that display similar EPR signals.

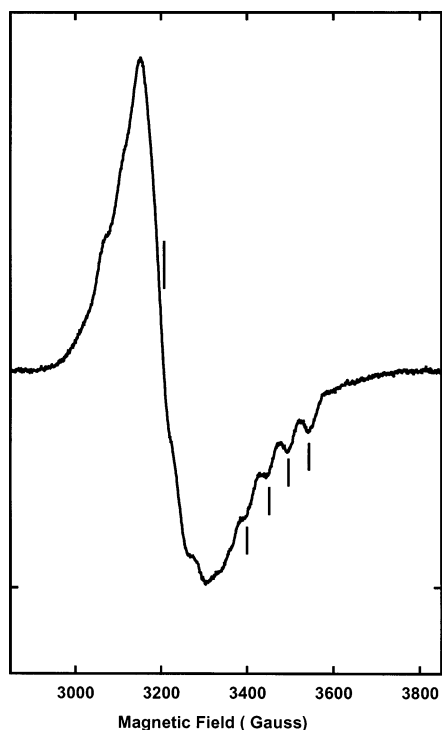


**Figure 7.** EPR spectrum of methylmalonyl-CoA mutase frozen under steady-state conditions with methylmalonyl-CoA mutase. Axial spectra similar to the spectrum seen with methylmalonyl-CoA mutase have also been observed with glutamate mutase and methyleneglutarate mutase in the presence of their respective substrates. The low-field line markers indicate the crossover  $g$  value of 2.11, and the high-field markers point to the nitrogen hyperfine lines.

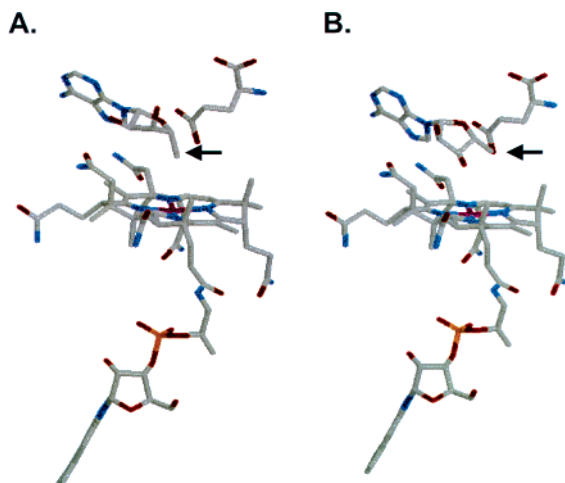


**Figure 8.** Ribose pseudorotation as a means of radical shuttling between the cofactor and substrate in glutamate mutase. (A) In the  $C2'$ -endo conformation, the  $C5'$  of deoxyadenosine is directed toward the cobalt. (B) In the  $C3'$ -endo conformation, the  $C5'$  of deoxyadenosine is directed toward the substrate. The arrows point to the  $C5'$  carbon. The figure was generated using the PDB file 1I9C.

In the crystal structure of glutamate mutase with bound AdoCbl and glutamate, the ribose ring is found to exhibit two conformations,  $C2'$ -endo and  $C3'$ -endo (Figure 8).<sup>37</sup> This conformational toggling has dramatic consequences on the distance between  $C5'$  of deoxyadenosine and cobalt and on the orientation of  $C5'$ , where the deoxyadenosyl radical is localized. Thus,  $C5'$  is positioned above the cobalt in the  $C2'$ -

endo conformer (Figure 8A), but it is directed toward the substrate hydrogen atom destined for abstraction in the  $C3'$ -endo conformer (Figure 8B). The energy barrier for ribose pseudorotation toggling between the two minimum energy conformations,  $C2'$ -endo and  $C3'$ -endo, is very low. This radical delivery mechanism represents an elegant solution to the problem of controlling radical trajectories and suppressing unwanted atom abstractions that would lead to inactivation.

#### IV. The Rearrangement Reaction

The aspect of AdoCbl-dependent reactions that is least well understood and continues to foment debate is the mechanism of the rearrangement step itself. It has also been the most neglected aspect of mechanistic investigations on the respective enzymes, although insights emanating from crystal structures have served as important guides in mutagenesis studies that are beginning to illuminate this issue. While the simplest mechanism, i.e., a direct radical rearrangement, can be entertained for the enzymes catalyzing migration of an  $sp^2$  carbon, it cannot for glutamate mutase, which is apparently singular in its ability to mobilize an  $sp^3$ -hybridized radical. For many years, most of the AdoCbl-dependent isomerizations represented reactions without chemical precedent for migrations in the free radical stage. However, this gap has now been filled with chemical models for rearrangements of other groups and complemented by theoretical studies that are discussed below.

Alternatives to a direct rearrangement pathway are presented in Scheme 2, and include rearrangements via carbanion (a) or carbonium ion (b) intermediates, via fragmentation/recombination (d), or via an organocobalt adduct (e) formed by the transient recombination of the substrate radical and cob(II)alamin. The carbanion and carbonium ion pathways necessitate electron transfer between the substrate radical and cob(II)alamin, and neither is supported by rapid reaction kinetic data, which do not reveal oxidation state changes in the initially formed cob(II)alamin.<sup>24,54</sup> Furthermore, the carbocation pathway is handicapped by the unfavorable redox potential for the  $Co^{2+}/Co^+$  couple of cobalamin ( $\sim -640$  mV for the free cofactor in neutral aqueous solution<sup>70</sup>). The organocobalt adduct would appear to be precluded by the crystal structures of methylmalonyl-CoA mutase<sup>16,18</sup> and glutamate mutase,<sup>37</sup> as well as by EPR spectroscopy,<sup>65</sup> which reveals the interrational distance between cob(II)alamin and the substrate-derived radical to be too great to afford their collapse. The fragmentation/recombination pathway provides a route for rearrangement without electron transfer to the cobalt and is germane to the glutamate mutase-catalyzed reaction as discussed below.

Migration of the carbon skeleton during conversion of substrate to product radicals occurs with inversion of stereochemistry at the respective carbon centers in glutamate mutase and 2-methyleneglutarate mutase<sup>7</sup> but with retention of configuration for methylmalonyl-CoA mutase<sup>58,71</sup> and isobutyryl-CoA mutase.<sup>72</sup> Mechanistic proposals for these enzymes must



therefore take into account these stereochemical constraints.

### A. Chemical and Computational Models

The design and testing of chemical models for B<sub>12</sub>-dependent isomerases was an active field of investigation in the 1980s and has been the subject of several reviews;<sup>73,74</sup> only select chemical models are discussed here. Historically, the 1,2 migration corresponding to the methyleneglutarate mutase-catalyzed reaction, i.e., of a vinyl group (Scheme 1), was the only one to be observed directly in model radicals for many years.<sup>75</sup> A chemical model for the methylmalonyl-CoA mutase-catalyzed reaction was reported by Halpern's group, in which the spontaneous migration of the thioester moiety in the radical, EtSC(=O)C(CH<sub>3</sub>)-(CH<sub>2</sub>)CO<sub>2</sub>EtS, was observed.<sup>76,77</sup> The rate constant for this rearrangement was ca. 40-fold lower than the  $k_{\text{cat}}$  for the methylmalonyl-CoA mutase reaction. The thermodynamic parameters for this rearrangement were estimated to be  $\Delta H^\ddagger = 13.8 \pm 0.2 \text{ kcal mol}^{-1}$  and  $\Delta S^\ddagger = -11 \text{ cal mol}^{-1} \text{ K}^{-1}$ , corresponding to  $\Delta G^\ddagger = 17.2 \text{ kcal mol}^{-1}$  at 37 °C. The discrepancy between the rearrangement rate in the chemical model and the enzyme-catalyzed reaction indicates the role that active-site residues may play in assisting this reaction. In this light, it is interesting to note that computational studies lend support to the efficacy of proton transfer in lowering the rearrangement transition state in these 1,2 migration reactions.<sup>56,78,79</sup> Significantly, a monotonic lowering of the energetic barrier from 11.2 to 2.4 kcal mol<sup>-1</sup> was predicted for the degenerate rearrangement of the 3-propanal radical, representing a simplified model of the methylmalonyl-CoA radical.<sup>78</sup>

High-level ab initio molecular orbital calculations predict that the energetic barrier for the fragmentation/recombination pathway for a methylmalonyl-related radical (in which the CoA group is replaced by hydrogen) is higher (17.1 kcal mol<sup>-1</sup>) than that for the intramolecular addition/elimination pathway (15.4 kcal mol<sup>-1</sup>) and demonstrate that proton transfer can further reduce the barrier in the latter pathway.<sup>79</sup> Similarly, calculations on the rearrangement of the methyleneglutaryl radical to the 3-methylitaconic acid radical reveal that the fragmentation/recombination barrier is higher (by >24 kcal mol<sup>-1</sup>) than that for the intramolecular pathway, which is further facilitated by protonation.<sup>80</sup> Thus, the simplest mechanism for the rearrangements involving migration of unsaturated carbons is an enzyme-assisted direct intramolecular pathway involving a cyclopropyl intermediate or transition state (Scheme 3).

The reaction catalyzed by glutamate mutase is unique because a saturated carbon center, the glycy radical, relocates. In this situation, a direct pathway involving a three-membered cyclic transition state is not chemically plausible, and an alternative mechanism, i.e., fragmentation/recombination, has to be entertained (Scheme 3).<sup>7</sup> In this mechanism, cleavage of the initially formed glutamyl radical results in formation of a 2-glyciny radical and acrylate. Addition of the glycinyl radical to the *Re* face of acrylate

leads to the product methylaspartyl radical with the requisite stereochemical inversion. Ab initio molecular orbital calculations predict that the energetic barrier for this pathway is unacceptably high if the glutamyl radical is either protonated (44 kcal mol<sup>-1</sup>) or unprotonated (23 kcal mol<sup>-1</sup>), relative to the size of the highest barrier (14–18 kcal mol<sup>-1</sup>) calculated from the  $k_{\text{cat}}$  for this reaction.<sup>56</sup> This results from loss of captodative stabilization of the glycy radical due to protonation of the amino group or deprotonation of the carboxylic group. However, the fragmentation barrier for the neutral substrate radical is considerably lower (14 kcal mol<sup>-1</sup>) and lies within the range estimated for glutamate mutase. Thus, enzymatic assistance by general acid/base catalysis to deprotonate the NH<sub>3</sub><sup>+</sup> group and protonate the COO<sup>-</sup> group of the migrating glycy radical is expected to facilitate the rearrangement reaction.<sup>56</sup> The relevance of this computational study to the active-site environment in glutamate mutase is discussed below. Rapid quench flow experiments have provided evidence for the fragmentation mechanism by demonstrating formation of acrylate at a kinetically competent rate.<sup>81</sup>

### B. Comparison of Active Sites of Methylmalonyl-CoA Mutase and Glutamate Mutase

While the choice of rearrangement pathways within the family of carbon skeleton isomerases is likely to differ depending on the nature of the migrating group, computational studies predict that enzymatic assistance by partial proton transfer may be a common mechanism. The active-site structures of methylmalonyl-CoA mutase and glutamate mutase are compared in Figure 6, and reveal a wealth of polar residues lining the substrate-binding pockets. In methylmalonyl-CoA mutase, the charged carboxyl group is neutralized by R207 and Y89, and the thioester oxygen is within hydrogen-bonding distance of H244. In the active site of glutamate mutase, three arginine residues, R66, R100, and R149 (described as arginine claws<sup>40</sup>), dock the two carboxyls at either end of the molecule, while E171 is within hydrogen-bonding distance to the  $\alpha$ -amino group. The multiple electrostatic interactions between active-site residues and the substrates additionally serve to lock in the reactive radical intermediates and prevent their diffusive escape. Computational studies predict that a 1–2 kcal mol<sup>-1</sup> penalty on the rearrangement barrier is incurred by loss of each of the hydrogen-bonding interactions between active-site residues (Y89, Q197, and H244) and substrate in methylmalonyl-CoA mutase.<sup>82</sup> Thus, together, they could provide a significant catalytic benefit for the reaction.

The location of H244 in the active site of methylmalonyl-CoA mutase suggests a potential role for it in facilitation of the rearrangement reaction via partial proton transfer. Mutation of this residue to a glycine, alanine, or glutamine<sup>83,84</sup> results in a 10<sup>2</sup>–10<sup>3</sup>-fold diminution of  $k_{\text{cat}}$ . The pH versus activity profile, characterized for the H244G mutant, exhibits loss of one of two kinetic pK<sub>a</sub>'s seen in the wild-type enzyme. Since loss of this pK<sub>a</sub> (8.4) is associated with

mutation at a single residue, it is assigned to H244.<sup>83</sup> The structure of the H244A mutant has been determined and does not reveal structural alterations other than at the site of mutagenesis.<sup>84</sup> Tritium partitioning from the 5' position of AdoCbl to the substrate or product was found to be dependent on which was used to initiate the reaction, in contrast to the wild-type enzyme, where the partition ratio showed directional independence, indicating a low barrier to rearrangement.<sup>84</sup> These results are consistent with an increase in the rearrangement barrier incurred by mutation of H244. Remarkably, mutation of H244 increases the oxidative susceptibility of the methylmalonyl-CoA mutase-catalyzed reaction, and interception of cob(II)alamin occurs every 22 turnovers, leading to inactivation.<sup>83,84</sup> Thus, in addition to assisting the rearrangement reaction, this residue plays a key role in shielding radical intermediates from the efficient radical quencher, oxygen.

Mutation of E171 in glutamate mutase to glutamine results in a 50-fold decrease in  $k_{\text{cat}}$  and a pH independence of  $V_{\text{max}}$ , in contrast to wild-type enzyme, in which the acidic limb of the pH dependence curve titrates with a  $\text{p}K_{\text{a}}$  of 6.6.<sup>85</sup> In addition, the overall deuterium isotope effect is further suppressed from  $^{\text{D}}V = 4.6 \pm 0.06$  to  $2.1 \pm 0.2$  in the mutant. These results are consistent with a model in which E171 functions as a general base to deprotonate the amino group of the substrate and thereby facilitates formation of a glycol radical intermediate during fragmentation.

## V. Qualitative Free Energy Profiles

Kinetic and thermodynamic characterization of the reactions catalyzed by wild-type and mutant isomerases are beginning to shed light on the qualitative free energy profiles of the two best-studied enzymes, methylmalonyl-CoA mutase and glutamate mutase. It is important to emphasize that these are at best qualitative because our understanding of the detailed kinetic mechanism of these reactions is far from complete. In the reaction catalyzed by methylmalonyl-CoA mutase, the free energy profile (Figure 9) can be compiled from the following pieces of experimental data. Binding of the substrate, methylmalonyl-CoA, is exothermic ( $\Delta G = -5.2 \text{ kcal mol}^{-1}$  at  $37^\circ\text{C}$ <sup>57</sup>), and the coupled homolysis/substrate radical generation steps are rapid, i.e.,  $>10$ -fold greater than  $k_{\text{cat}}$ .<sup>24</sup> The overall deuterium isotope effect associated with this reaction is suppressed ( $^{\text{D}}V = 5-6$ <sup>42,58</sup>) and significantly smaller than the deuterium isotope effect on the hydrogen atom abstraction from substrate (35.6 at  $20^\circ\text{C}$ <sup>62</sup>), indicating that the hydrogen-transfer steps are not completely rate limiting. The tritium partitioning ratio from the C5' position of AdoCbl to substrate and product is independent of the direction of the catalyzed reaction, revealing that the barrier to interconversion of substrate and product radicals is low.<sup>60</sup> Finally, the predominance of AdoCbl ( $\sim 80\%$ ) over cob(II)alamin ( $\sim 20\%$ ) under steady-state conditions<sup>24</sup> suggests that product release is rate determining.

Compilation of a qualitative free energy profile for the reaction catalyzed by glutamate mutase (Figure

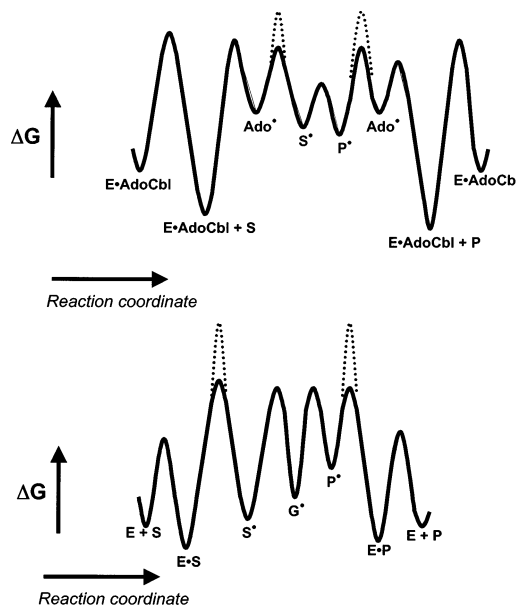


**Figure 9.** Qualitative free energy profiles for the carbon skeleton rearrangements catalyzed by methylmalonyl-CoA mutase (A) and glutamate mutase (B). In A, the methylmalonyl-CoA mutase-catalyzed reaction, S $\cdot$  and P $\cdot$  refer to the substrate (methylmalonyl-CoA) and product (succinyl-CoA) radicals, respectively. The profile was adapted from ref 57. In the glutamate mutase reaction, S $\cdot$ , G $\cdot$ , and P $\cdot$  refer to the substrate (glutamyl), glycol, and product (methylaspartyl) radicals, respectively. The profile was adapted from ref 86.

9B) is guided by the following pieces of experimental data. The coupled homolysis/substrate radical generation steps are rapid and characterized by large deuterium isotope effects ( $^{\text{D}}V \approx 30$  at  $10^\circ\text{C}$ <sup>54</sup>). The overall deuterium isotope effects with glutamate ( $^{\text{D}}V = 3.9$ ) and methylaspartate ( $^{\text{D}}V = 6.3$ ) are suppressed, indicating that the hydrogen-transfer steps are not rate determining. Tritium from the 5' carbon of AdoCbl partitions in an  $\sim 1:1$  ratio between substrate and product and is independent of the direction in which the reaction proceeds.<sup>86</sup> These results indicate that the energetic barriers for the transfer of tritium from 5'-deoxyadenosine to the substrate and product radicals are almost equal and that the interconversion of glutamyl and methylaspartyl radicals is fast relative to tritium transfer.<sup>86</sup> Absence of burst kinetics is interpreted as evidence against the product release step being rate limiting.<sup>87</sup> In the presence of glutamate, the slow step is postulated to be recombination of the glycol radical and acrylate, whereas in the reverse direction, the first slow step is formation of the methylaspartyl radical followed by a second slow step, i.e., recombination of the glycol radical and acrylate.<sup>81</sup> However, this interpretation appears to be at odds with the predominance of AdoCbl over cob(II)alamin under steady-state conditions in the presence of either glutamate or methylaspartate,<sup>54</sup> and the results from tritium partitioning experiments that indicate interconversion of substrate and product radicals is fast relative to the tritium abstraction steps.<sup>86</sup> These discrepancies reflect our incomplete understanding of the reaction profiles.

## VI. Conclusions

The availability of relatively large amounts of recombinant protein in the past decade has driven studies on AdoCbl-dependent enzymes to a deeper level of inquiry. Crystal structures of two of the carbon skeleton isomerases reveal similarities in the overall molecular architecture and in the mode of B<sub>12</sub> binding but differences in the constellation of active-site residues that probably reflect evolutionary fine-tuning for different catalytic mechanisms. The structure of glutamate mutase has provided unexpected insights into how the cofactor-derived deoxyadenosyl radical shuttles between recombination and substrate (or product) radical generation via a conformational toggle of the ribose ring. This mechanism is likely to be general in AdoCbl-dependent enzymes, where the interradsical distance is in the 6–7 Å range. Kinetic studies have revealed the strategy that is used to control the radical generator, AdoCbl, i.e., by coupling of the homolysis and substrate radical generation steps. Kinetic isotope effect measurements provide strong evidence that the hydrogen-transfer step between substrate and cofactor occurs via quantum mechanical tunneling in methylmalonyl-CoA mutase and glutamate mutase and reveals yet another catalytic strategy deployed by these enzymes.

Kinetic and mutagenesis studies are beginning to shed light on details of the rearrangement reaction and the roles of individual active-site residues in the remarkable stabilization of radical intermediates and suppression of radical interception by side reactions. Similar approaches are likely to be productive for elucidating the mechanism of the trillion-fold acceleration of the Co–carbon bond and the stereochemical control of the reactions. Finally, the synergistic interplay between computational and experimental studies continues to fuel the designing and testing of models to explain the chemical and energetic details of the reaction coordinates for the different carbon skeleton isomerases.

## VII. Acknowledgment

This work was supported by a grant from the National Institutes of Health (DK45776). R.B. is an Established Investigator of the American Heart Association.

## VIII. References

- Barker, H. A.; Weissbach, H.; Smyth, R. D. *Proc. Natl. Acad. Sci. U.S.A.* **1958**, *44*, 1093–1097.
- Lenhert, P. G.; Hodgkin, D. C. *Nature (London)* **1961**, *192*, 937–938.
- Todd, L. In *Vitamin B<sub>12</sub>*; Walter de Gruyter: Berlin, 1979.
- Banerjee, R. *Biochemistry* **2001**, *40*, 6191–6198.
- Marsh, E. N.; Drennan, C. L. *Curr. Opin. Chem. Biol.* **2001**, *5*, 499–505.
- Banerjee, R. *Chem. Biol.* **1997**, *4*, 175–186.
- Buckel, W.; Golding, B. T. *Chem. Soc. Rev.* **1996**, *26*, 329–337.
- Fenton, W. A.; Rosenberg, L. E. In *The metabolic and molecular bases of inherited disease*; Scriver, C. R., Beaudet, A. L., Sly, W. S., Valle, D., Eds.; McGraw-Hill: New York, 1995.
- Leutbecher, U.; Albracht, S. P. J.; Buckel, W. *FEBS Lett.* **1992**, *307*, 144–146.
- Ratnatilleke, A.; Vrijbloed, J. W.; Robinson, J. A. *J. Biol. Chem.* **1999**, *274*, 31679–31685.
- Beatrix, B.; Zelder, O.; Linder, D.; Buckel, W. *Eur. J. Biochem.* **1994**, *221*, 101–109.
- Roy, I.; Leadlay, P. F. *J. Bacteriol.* **1992**, *174*, 5763–5764.
- Haller, T.; Buckel, T.; Retej, J.; Gerlt, J. A. *Biochemistry* **2000**, *39*, 4622–4629.
- Charles, T. C.; Aneja, P. *Gene* **1999**, *226*, 121–127.
- Frey, P. A.; Essenberg, M. K.; Abeles, R. H. *J. Biol. Chem.* **1967**, *242*, 5369–5377.
- Mancia, F.; Keep, N. H.; Nakagawa, A.; Leadlay, P. F.; McSweeney, S.; Rasmussen, B.; Bösecke, P.; Diat, O.; Evans, P. R. *Structure* **1996**, *4*, 339–350.
- Reitzer, R.; Gruber, K.; Jögl, G.; Wagner, U. G.; Bothe, H.; Buckel, W.; Kratky, C. *Struct. Fold. Des.* **1999**, *7*, 891–902.
- Mancia, F.; Evans, P. *Structure* **1998**, *6*, 711–720.
- Mancia, F.; Smith, G. A.; Evans, P. R. *Biochemistry* **1999**, *38*, 7999–8005.
- Base-on AdoCbl refers specifically to dimethylbenzimidazole coordination at the lower axial position. AdoCbl and AdoCbl-GDP are cofactor analogues and denote 5'-deoxyadenosylcobinamide and 5'-deoxyadenosylcobinamide guanosine diphosphate, respectively.
- Finke, R. G.; Hay, B. P. *Inorg. Chem.* **1984**, *23*, 3041–3043.
- Brown, K. L.; Hakimi, J. M. *J. Am. Chem. Soc.* **1984**, *106*, 7894–7899.
- Hay, B. P.; Finke, R. G. *J. Am. Chem. Soc.* **1987**, *109*, 8012–8018.
- Padmakumar, R.; Padmakumar, R.; Banerjee, R. *Biochemistry* **1997**, *36*, 3713–3718.
- Chemaly, S. M.; Pratt, J. M. *J. Chem. Soc., Dalton Trans.* **1980**, 2274–2281.
- Halpern, J.; Kim, S.-H.; Leung, T. W. *J. Am. Chem. Soc.* **1984**, *106*, 8317–8319.
- Marzilli, L. G.; Toscano, J.; Randaccio, L.; Bresciani-Pahor, N.; Calligaris, M. *J. Am. Chem. Soc.* **1979**, *101*, 6754–6756.
- Ng, F. T. T.; Rempel, G. L.; Halpern, J. *J. Am. Chem. Soc.* **1982**, *104*, 621–623.
- Geno, M. K.; Halpern, J. *J. Am. Chem. Soc.* **1987**, *109*, 1238–1240.
- Kräutler, B.; Konrat, R.; Stupperich, E.; Gerald, F.; Gruber, K.; Kratky, C. *Inorg. Chem.* **1994**, *33*, 4128–4139.
- Padmakumar, R.; Taoka, S.; Padmakumar, R.; Banerjee, R. *J. Am. Chem. Soc.* **1995**, *117*, 7033–7034.
- Zelder, O.; Beatrix, B.; Kroll, F.; Buckel, W. *FEBS Lett.* **1995**, *369*, 252–254.
- Marsh, E. N. G.; Holloway, D. E. *FEBS Lett.* **1992**, *310*, 167–170.
- Yamanishi, M.; Yamada, S.; Muguruma, H.; Murakami, Y.; Tobimatsu, T.; Ishida, A.; Yamauchi, J.; Toraya, T. *Biochemistry* **1998**, *37*, 4799–4803.
- Abend, A.; Bandarian, V.; Nitsche, R.; Stupperich, E.; Retej, J.; Reed, G. H. *Arch. Biochem. Biophys.* **1999**, *370*, 138–141.
- Lawrence, C. C.; Gerfen, G. J.; Samano, V.; Nitsche, R.; Robins, M. J.; Retej, J.; Stubbe, J. *J. Biol. Chem.* **1999**, *274*, 7039–7042.
- Gruber, K.; Reitzer, R.; Kratky, C. *Angew. Chem., Int. Ed.* **2001**, *40*, 3377–3380.
- Sirovatka, J. M.; Finke, R. G. *J. Am. Chem. Soc.* **1997**, *119*, 3057–3067.
- Chen, H. P.; Marsh, E. N. *Biochemistry* **1997**, *36*, 7884–7889.
- Buckel, W.; Bröker, G.; Bothe, H.; Pierik, A. J. In *Chemistry and Biochemistry of B<sub>12</sub>*; Banerjee, R., Ed.; John Wiley and Sons: New York, 1999.
- Vlasie, M. D.; Chowdhury, S.; Banerjee, R. *J. Biol. Chem.* **2002**, *277*, 18523–18527.
- Chowdhury, S.; Thomas, M. G.; Escalante-Semerena, J. C.; Banerjee, R. *J. Biol. Chem.* **2001**, *276*, 1015–1019.
- Chowdhury, S.; Banerjee, R. *Biochemistry* **1999**, *38*, 15287–15294.
- Tollinger, M.; Konrat, R.; Hilbert, B. H.; Marsh, E. N. G.; Krautler, B. *Structure* **1998**, *6*, 1021–1033.
- Grate, J. H.; Schrauzer, G. N. *J. Am. Chem. Soc.* **1979**, *101*, 4601–4611.
- Glusker, J. P. In *B<sub>12</sub>*; Dolphin, D., Ed.; Wiley: New York, 1982; Vol. 1.
- Brown, K. L.; Brooks, H. B. *Inorg. Chem.* **1991**, *30*, 3420–3430.
- Dong, S.; Padmakumar, R.; Banerjee, R.; Spiro, T. G. *J. Am. Chem. Soc.* **1999**, *121*, 7063–7070.
- Dong, S.; Padmakumar, R.; Maiti, N.; Banerjee, R.; Spiro, T. G. *J. Am. Chem. Soc.* **1998**, *120*, 9947–9948.
- Dong, S.; Padmakumar, R.; Banerjee, R.; Spiro, S. *Inorg. Chim. Acta* **1998**, *270*, 392–398.
- Dong, S.; Padmakumar, R.; Banerjee, R.; Spiro, T. G. *J. Am. Chem. Soc.* **1996**, *118*, 9182–9183.
- Huhta, M. S.; Chen, H. P.; Hemann, C.; Hille, C. R.; Marsh, E. N. *Biochem. J.* **2001**, *355*, 131–137.
- Gaudemer, A.; Zybler, J.; Zybler, N.; Baran-Marszac, M.; Hull, W. E.; Fountoulakis, M.; König, A.; Wolfe, K.; Retej, J. *Eur. J. Biochem.* **1981**, *119*, 279–285.
- Marsh, E. N. G.; Ballou, D. P. *Biochemistry* **1998**, *37*, 11864–11872.
- Dybala-Defratyka, A.; Paneth, P. *J. Inorg. Biochem.* **2001**, *86*, 681–689.

- (56) Wetmore, S. D.; Smith, D. M.; Golding, B. T.; Radom, L. *J. Am. Chem. Soc.* **2001**, *123*, 7963–7972.
- (57) Chowdhury, S.; Banerjee, R. *Biochemistry* **2000**, *39*, 7998–8006.
- (58) Michenfelder, M.; Hull, W. E.; Retey, J. *Eur. J. Biochem.* **1987**, *168*, 659–667.
- (59) Taoka, S.; Padmakumar, R.; Grissom, C. H.; Banerjee, R. *Bioelectromagnetics* **1997**, *18*, 506–513.
- (60) Meier, T. W.; Thomä, N. H.; Leadlay, P. F. *Biochemistry* **1996**, *35*, 11791–11796.
- (61) Marsh, E. N. G. *Biochemistry* **1995**, *34*, 7542–7547.
- (62) Chowdhury, S.; Banerjee, R. *J. Am. Chem. Soc.* **2000**, *122*, 5417–5418.
- (63) Zhao, Y.; Such, P.; Retey, J. *Angew. Chem., Int. Ed. Engl.* **1992**, *31*, 215–216.
- (64) Padmakumar, R.; Banerjee, R. *J. Biol. Chem.* **1995**, *270*, 9295–9300.
- (65) Bothe, H.; Darley, D. J.; Albracht, S. P.; Gerfen, G. J.; Golding, B. T.; Buckel, W. *Biochemistry* **1998**, *37*, 4105–4113.
- (66) Beatrix, B.; Zelder, O.; Kroll, F.; Örlýgsson, G.; Golding, B. T.; Buckel, W. *Angew. Chem., Int. Ed. Engl.* **1995**, *34*, 2398–2401.
- (67) Keep, N. H.; Smith, G. A.; Evans, M. C. W.; Diakun, G. P.; Leadlay, P. F. *Biochem. J.* **1993**, *295*, 387–392.
- (68) Gerfen, G. F. *EPR spectroscopy of B<sub>12</sub>-dependent enzymes*; John Wiley and Sons: New York, 1999.
- (69) Zhao, Y.; Abend, A.; Kunz, M.; Such, P.; Retey, J. *Eur. J. Biochem.* **1994**, *225*, 891–896.
- (70) Lexa, D.; Saveant, J.-M. *Acc. Chem. Res.* **1983**, *16*, 235–243.
- (71) Michenfelder, M.; Retey, J. *Angew. Chem., Int. Ed. Engl.* **1986**, *25*, 366–367.
- (72) Moore, B. S.; Eisenberg, R.; Weber, C.; Bridges, A.; Nanz, D.; Robinson, J. A. *J. Am. Chem. Soc.* **1995**, *117*, 11285–11291.
- (73) Halpern, J. *Science* **1985**, *227*, 869–875.
- (74) Retey, J. In *Vitamin B<sub>12</sub> and B<sub>12</sub> Proteins*; Kräutler, B., Arigoni, D., Golding, B. T., Eds.; Wiley-VCH: Weinheim, 1998.
- (75) Effio, A.; Griller, D.; Ingold, K. U.; Beckwith, A. L. J.; Serelis, A. K. *J. Am. Chem. Soc.* **1980**, *102*, 1734–1736.
- (76) Wollowitz, S.; Halpern, J. *J. Am. Chem. Soc.* **1984**, *106*, 8319–8321.
- (77) Wollowitz, S.; Halpern, J. *J. Am. Chem. Soc.* **1988**, *110*, 3112–3120.
- (78) Smith, D. M.; Golding, B. T.; Radom, L. *J. Am. Chem. Soc.* **1999**, *121*, 1383–1384.
- (79) Smith, D. M.; Golding, B. T.; Radom, L. *J. Am. Chem. Soc.* **1999**, *121*, 9388–9399.
- (80) Smith, D. M.; Golding, B. T.; Radom, L. *J. Am. Chem. Soc.* **1999**, *121*, 1037–1044.
- (81) Chih, H.-W.; Marsh, E. N. G. *J. Am. Chem. Soc.* **2000**, *122*, 10732–10733.
- (82) Loferer, M. J.; Webb, B. M.; Grant, G. H.; Liedl, K. R. *J. Am. Chem. Soc.* **2003**, *125*, 1072–1078.
- (83) Maiti, N.; Widjaja, L.; Banerjee, R. *J. Biol. Chem.* **1999**, *274*, 32733–32737.
- (84) Thoma, N. H.; Evans, P. R.; Leadlay, P. F. *Biochemistry* **2000**, *39*, 9213–9221.
- (85) Madhavapeddi, P.; Marsh, E. N. *Chem. Biol.* **2001**, *8*, 1143–1149.
- (86) Chih, H. W.; Marsh, E. N. *Biochemistry* **2001**, *40*, 13060–13067.
- (87) Chih, H. W.; Marsh, E. N. *Biochemistry* **1999**, *38*, 13684–13691.

CR0204395